Multiphoton inner-shell ionization of the carbon atom

H. F. Rey* and H. W. van der Hart

Centre for Theoretical Atomic, Molecular and Optical Physics, School of Mathematics and Physics, Queen's University Belfast, Belfast BT7 1NN, United Kingdom

(Received 6 May 2015; published 21 July 2015)

We apply time-dependent R-matrix theory to study inner-shell ionization of C atoms in ultrashort high-frequency light fields with a photon energy between 170 and 245 eV. At an intensity of 10^{17} W/cm^2, ionization is dominated by single-photon emission of a 2ℓ electron, with two-photon emission of a $1s$ electron accounting for about 2–3% of all emission processes, and two-photon emission of 2ℓ contributing about 0.5–1%. Three-photon emission of a $1s$ electron is estimated to contribute about 0.01–0.03%. Around a photon energy of 225 eV, two-photon emission of a $1s$ electron, leaving C^+ in either $1s2s2p^3$ or $1s2p^4$, is resonantly enhanced by intermediate $1s2s^22p^3$ states. The results demonstrate the capability of time-dependent R-matrix theory to describe inner-shell ionization processes including rearrangement of the outer electrons.

DOI: 10.1103/PhysRevA.92.013417 PACS number(s): 32.80.Rm, 31.15.A−

I. INTRODUCTION

Over the past decade, great strides have been made in the development of free-electron lasers operating in the VUV x-ray regime. Several free-electron lasers operating in the XUV x-ray regime have become available to the community in recent years, for example, FLASH [1], LCLS [2], and SACLA [3]. These facilities have demonstrated their potential for opening new areas of atomic, molecular, and optical physics, for example through the study of Auger resonances which cannot be excited by a single photon [4], multiphoton sequential ionization of Xe up to Xe^{36+} at a photon energy of 1.5 keV [5], and multiphoton multiple ionization of N_2 [6].

Photoionization in high-frequency laser fields tends to be dominated by the innermost electron that can be ejected. However, the outer electrons will also experience the light field and can therefore still absorb a photon. Hence, a full description of the atomic or molecular response should consider all electrons that could possibly be affected by the laser field. In addition, outer electrons do not necessarily remain in their original orbital when an inner electron is removed from the system. The potential seen by the outer electrons may change suddenly, leading to shakeup excitation of the outer electrons.

A full theoretical or computational study of the interaction between high-frequency laser light and atoms therefore requires a method which can describe the simultaneous response of many electrons to the laser field. Several such methods have been developed in recent years, such as the time-dependent configuration-interaction singles (TDCIS) method, which has recently been applied to study above-threshold ionization for light elements in the hard x-ray regime [7]; a Green's function technique, algebraic diagrammatic construction (ADC), which has been applied to study fast dynamics in glycine using laser pulses at a photon energy of 275 eV [8]; and time-dependent R-matrix theory, which has been used to study the competition between emission of a $2s$ and a $2p$ electron in C in the UV regime [9].

In the present study, we continue our study of the response of C atoms to laser light by investigating the photon energy range between 170 and 245 eV. The response of the carbon atom is of particular interest as it is the prime constituent of biological molecules. The removal of inner electrons from a carbon atom can provide new insight into molecular systems. For example, in [10], it was demonstrated that the removal of a $1s$ electron from the carbon atom in methane could be exploited experimentally to extract information about the molecular geometry. In [8], it was also proposed that dynamics in ionized glycine could be studied in a pump-probe scheme where the probe pulse excites a localized $1s$ electron of C to the orbital in which a hole is created by the pump pulse. A photon energy of 275–280 eV was suggested for this purpose. Advances in laser technology have very recently been exploited to generate individual subfemtosecond pulses in this photon energy range [11]. Thus, it is of interest to investigate ultrafast dynamics involving inner-shell electrons.

As a first step towards the treatment of short laser pulses at a photon energy of 284 eV [11], we compare in the present study emission of the inner $1s$ electron with emission of the outer $2s$ or $2p$ electrons for the photon energy range between 170 and 245 eV. Numerical studies of ultrafast dynamics at 284 eV involving the C atom will require great care with the pulse shape to ensure that inner-shell ionization processes are not dominated by direct single-photon emission arising from the outer edges of the pulse bandwidth. In the present photon energy range, emission of a $1s$ electron requires absorption of (at least) two photons, whereas the emission of a $2s$ or $2p$ electron requires absorption of a single photon only. This comparison is similar to a previous comparison of two-photon emission of the $1s$ electron versus one- and two-photon emission of the outer $2s$ electron using the R-matrix Floquet approach for Li^- [12] or the $1s2s\,{}^1S$ state in He [13].

To study the response of the carbon atom, we use the recently developed R matrix with time dependence (RMT) approach [14–16]. It combines the capability of R-matrix theory to describe a wide range of processes in general atomic systems [17–19] with the computational capability of the HELIUM approach [20]. The combination of these two techniques has enabled the determination of time delays

*hreypereira01@qub.ac.uk

in Ne [16], and high-order harmonic generation at mid-IR wavelengths [21]. For these studies, relatively little atomic structure was taken into account. By adopting an R matrix with pseudostates philosophy [22] or an intermediate-energy R-matrix approach [23], we have recently demonstrated that the RMT codes can also be used for the study of double-photoionization processes [24,25]. To describe the double continuum accurately, extensive atomic structure needs to be taken into account. The success of these latter studies suggests that the RMT approach is capable of treating atoms in strong fields with a detailed description of atomic structure.

In the present study, we wish to explore the application of RMT theory to a case where electrons can be ejected from different shells with significantly different binding energy. This application poses new demands on the computational accuracy. The continuum needs to be accurate up to very high energies to describe relevant above-threshold ionization processes involving outer electrons. This has the computational consequence of increasing the roundoff error in matching the wave function at the boundary between the inner and outer R-matrix regions, where the description of the ejected electron changes from basis-set techniques to finite-difference methods. Hence, the application of the RMT approach to inner-shell processes presents new demands on the computer codes.

In Sec. II, we give a short overview of the RMT approach. We also provide a brief description of the basis set used to describe the C atom, and the laser pulse. The results are presented in Sec. III with an emphasis on the competition between the multiphoton emission of an inner $1s$ electron and single- and multiphoton emission of an outer 2ℓ electron.

II. COMPUTATIONAL METHODS

Time-dependent R-matrix theory is the extension of the standard R-matrix approach [19] to the solution of the time-dependent Schrödinger equation [14–18,26]. Although the initial applications of time-dependent R-matrix theory described electrons restricted to a finite region surrounding the nucleus [17,18], subsequent implementations adopted the standard R-matrix concept of division of space into two distinct regions: an inner region in which all electrons are close to the nucleus, and an outer region in which one electron has moved well away from the others. In the original formulation of time-dependent R-matrix theory, an R-matrix propagation scheme was employed to propagate the wave function [26]. This approach relies on the solution of systems of equations throughout the calculation, and as a consequence calculation time increases rapidly with an increase in atomic structure.

The most recent implementation of time-dependent R-matrix theory is RMT [15,16]. In this approach, the wave function in the inner region is described in terms of a standard R-matrix basis with a B-spline representation of the continuum orbitals. The wave function in the outer region is described in terms of a direct product of a residual-ion state coupled with a finite-difference representation of the wave function for the outer electron. Near the boundary between the inner and outer regions, the wave function must be shared by the inner and outer regions. This is achieved through evaluation of the inner-region wave function on an outer-region grid extension into the inner region for use by the outer region. The outer-region wave function information needed by the inner region consists of spatial derivatives of the outer-region wave function at the inner-region boundary.

The main advantage of the RMT approach over the previous implementation is its improved accuracy and numerical efficiency. Whereas the previous implementation used a low-order Crank-Nicolson propagator, the RMT approach uses a high-order Arnoldi propagator [20]. This replaces a solution of a system of linear equations by repeated matrix-vector multiplications, which may reduce numerical error in the time and spatial propagation of the wave function. Since the Arnoldi propagator is dominated by matrix-vector multiplications, the RMT codes can be parallelized more efficiently, so that calculations exploiting in excess of 2000 cores are feasible.

In the present study, we aim to investigate inner-shell ionization processes involving the carbon atom. We are thus interested in residual-ion states with a hole in the $1s$ shell. Within the R-matrix codes, residual-ion states are retained in order of energy. As a consequence, all possible residual-ion states with a filled $1s^2$ shell are included prior to inclusion of the residual-ion states with a hole in the $1s$ shell. In order to limit the scale of the calculations, we therefore adopt a minimal basis for the description of carbon. The atom is described using only the $1s$, $2s$, and $2p$ Hartree-Fock orbitals of singly ionized carbon [27]. We then use these orbitals to build all possible singly charged residual-ion states, i.e., all states belonging to the $1s^2 2s^2 2p$, $1s^2 2s 2p^2$, $1s^2 2p^3$, $1s 2s^2 2p^2$, $1s 2s 2p^3$, and $1s 2p^4$ configurations of C^+. The neutral-atom basis then contains all combinations of these residual-ion states with a set of B-spline-based continuum orbitals up to a maximum total angular momentum $L_{\max} = 5$. We use a total of 125 B splines of order 9 to build these continuum orbitals. This basis also includes so-called correlation functions made of all combinations for six electrons across the $1s$, $2s$, and $2p$ orbitals with at least one electron in $1s$. The inner-region boundary is set to $27a_0$.

The application of RMT theory using this basis set to describe the atom poses a new challenge: a challenge that applies to all studies of inner-shell ionization processes. To describe all ionization processes properly, a good description of the continuum is needed for emission of both inner and outer electrons, including multiphoton emission processes. Multiphoton emission of outer electrons, in particular, can lead to very high continuum energies. An extensive expansion of the continuum is therefore required in the inner region, which allows for the description of rapidly oscillating continuum functions. As a consequence, the so-called knot points of the B-spline basis set are more closely spaced than in a calculation for outer electrons only: 125 B splines in the present case, compared to 70 for the outer-electron calculation [9]. The introduction of the Bloch operator to maintain Hermiticity of the Hamiltonian in the inner region then generates eigenfunctions with large eigenvalues (up to 200 keV) which are sharply peaked near the R-matrix boundary. Since these functions are peaked near the boundary, they need to be retained in the calculations. However, the effect of the large eigenvalues must be compensated for through the connection between the inner region and the outer region. Hence, a cancellation of terms involving large energies occurs at every stage of

TABLE I. Final-state populations in the outer region for ground-state C atoms irradiated by an ultrashort laser pulse with a central photon energy of 190 and 245 eV at different peak laser intensities. The ground state of C has even parity. The notation 1.54(−6) indicates 1.54×10^{-6}. The populations are averaged over initial orbital magnetic quantum number M_L.

Channel subset	Photon energy (eV)	Peak intensity (W/cm^2)				
		10^{14}	10^{15}	10^{16}	10^{17}	10^{18}
C^+ 2ℓ emission, odd parity	190	3.89(−5)	3.89(−4)	3.87(−3)	3.64(−2)	2.07(−1)
C^+ 2ℓ emission, even parity	190	2.45(−10)	2.45(−8)	2.45(−6)	2.45(−4)	2.68(−2)
C^+ $1s$ emission, even parity	190	6.59(−10)	6.59(−8)	6.55(−6)	6.18(−4)	3.66(−2)
C^+ $1s$ emission, odd parity	190	2.55(−9)	2.55(−8)	2.57(−7)	7.92(−6)	3.16(−3)
C^+ 2ℓ emission, odd parity	245	1.29(−5)	1.28(−4)	1.28(−3)	1.24(−2)	
C^+ 2ℓ emission, even parity	245	5.05(−11)	5.05(−9)	5.02(−7)	4.76(−5)	
C^+ $1s$ emission, even parity	245	3.19(−10)	3.18(−8)	3.16(−6)	2.96(−4)	
C^+ $1s$ emission, odd parity	245	3.90(−7)	3.90(−6)	3.90(−5)	3.89(−4)	

the calculation. This cancellation can be a prime source of numerical error, and extra care therefore needs to be taken to ensure numerical stability of the calculations, for example through a significant reduction of the time step in the calculation.

Within the RMT approach, the light field is assumed to be linearly polarized and described within the length form of the dipole approximation due to the necessity to restrict the residual-ion basis [28]. The field is described by an ultrashort light pulse of eight cycles, including a three-cycle $\sin^2$ ramp-on and ramp-off, with two cycles at peak intensity. The photon energies in the present study range from 170 to 245 eV, so that a single photon suffices to eject an outer 2ℓ electron, but absorption of two photons is required to emit the $1s$ electron. The bandwidth of the pulse is about 40 eV (full width at half maximum) at a photon energy of 245 eV. After the pulse has ended, we propagate the wave function for another 42 cycles to ensure that all ejected electrons have entered the outer region. The time step used in the calculation is 0.012 as. The outer-region finite-difference grid has a spacing of $0.025a_0$ and extends out to a distance of $816a_0$. We use an Arnoldi propagator of order 10.

III. RESULTS

In the present study, we aim to investigate the competition between single-photon emission of a 2ℓ electron and two-photon emission of a $1s$ electron from a carbon atom in the photon energy range between 170 and 245 eV. Since the C ground state has $^3P^e$ symmetry, the initial state can have $M_L = -1$, 0, and 1. In all results presented, unless otherwise stated, we have averaged over the different initial M_L values. For nonzero initial M_L, the S symmetry is not available, whereas for zero M_L, radiative transitions with $\Delta L = 0$ are not allowed.

In Table I, we present final-state populations in the outer region for various subsets of photoemission channels when carbon is irradiated by a short pulse of 190- and 245-eV photons at various peak laser intensities. The table shows that the yield for odd-parity channels associated with emission of a 2ℓ electron scales approximately linearly with intensity between 10^{14} and 10^{17} W/cm^2. This indicates that these channels correspond to single-photon emission of an outer 2ℓ electron. The population in the even-parity channels associated with 2ℓ emission increases quadratically with intensity, and this population can thus be interpreted as two-photon above-threshold emission of a 2ℓ electron. Similarly, the population in the even-parity channels associated with $1s$ emission increases quadratically with intensity, and this population can be interpreted as two-photon emission of a $1s$ electron. Up to intensities of 10^{17} W/cm^{-2}, the assumption that perturbation theory applies is therefore not unreasonable, with deviations typically less than 7%.

At an intensity of 10^{18} W/cm^2, the assumption of perturbation theory certainly no longer holds. The single-photon emission yield for a 2ℓ electron increases by about a factor of 6 between 10^{17} W/cm^2. The two-photon emission yield for a $1s$ electron increases by about a factor of 60 between 10^{17} W/cm^2. In both cases, a reduction of about 40% from the perturbative result is observed. For two-photon emission of a 2ℓ electron, an additional increase in the yield of about 10% is seen. Total ionization has become substantial at 10^{18} W/cm^2, with about 27% of all atoms ionized within a short time. Hence, perturbation theory should no longer be expected to apply at this intensity. Perturbation theory could fail in different respects: an increase in importance of higher-order processes, and saturation of ionization, in combination with the very short duration of the XUV pulse (smaller than $2\pi/I_p$ with I_p the binding energy of the $2p$ electron). Also, the strength of the electric field will significantly change the actual potential seen by the outer electrons.

Table I shows, furthermore, that the population in odd-parity channels associated with $1s$ emission scales linearly with intensity at the lowest intensities for 190-eV photons and at all intensities for 245-eV photons. The reason for this is the large bandwidth of the ultrashort light pulse. The threshold for single-photon emission of the $1s$ electron in the present calculations is about 300 eV. (This threshold is not necessarily determined very accurately, since the lowest $1s$ emission threshold, $1s2s^22p^2\ ^4P^e$, is described using Hartree-Fock orbitals for the $1s^22s^22p$ ground state of C^+.) The ultrashort nature of the light pulse has sufficient bandwidth to allow single-photon ionization of a $1s$ electron to occur with a relative strength, compared to single-photon emission of a 2ℓ electron, of about 10^{-4} at 190 eV and about 3×10^{-2} at 245 eV. This increase with increasing photon energy is expected, as a larger photon energy will lead to a larger part of the bandwidth having sufficient energy to eject a $1s$ electron. At 245 eV, this bandwidth leads to dominance of single-photon

emission of a $1s$ electron over multiphoton emission even at an intensity of 10^{18} W/cm^2. However, at 190 eV, the population of the $1s$ emission channels with odd parity increases by a factor of 400 when the intensity is increased from 10^{17} to 10^{18} W/cm^2. This indicates that for this photon energy, three-photon processes start to become important near an intensity of 10^{17} W/cm^2. We can therefore obtain an estimate for three-photon emission of a $1s$ electron through comparison of the final-state populations obtained at intensities of 10^{14} and 10^{17} W/cm^2. This comparison gives a final-state population in $1s$ emission channels associated with three-photon absorption at an intensity of 10^{17} W/cm^2 of around 5.4×10^{-6}. This procedure to estimate above-threshold emission for the $1s$ electron can be carried out for photon energies up to about 220 eV.

The final-state populations in Table I have been averaged over M_L. Little difference is seen between the final-state populations for $M_L = 0$ and $M_L = \pm 1$, except for two-photon emission of the 2ℓ electrons, for which the $M_L = \pm 1$ yield is about 65% larger than the $M_L = 0$ population at 190 eV, a factor of 2 larger at 218 eV and 10% smaller at 245 eV. The most likely reason for the generally larger yield for $M_L = \pm 1$ is the presence of a $2p$ electron with $m_\ell = 0$ for the initial $M_L = 1$ level of the $^3P^e$ ground state of C, whereas no such electron is present for the initial $M_L = 0$ level. We note that this same principle was the reason for the relative increase in the emission of $2s$ electrons compared to $2p$ electrons in multiphoton ionization of C at 390 nm for $M_L = 0$ [9].

We can compare the ionization yields in the odd-parity channels with estimates of the photoionization cross sections in the various subshells [29]. The calculation we compare with also uses a very simple description for C. First we consider the results for a central photon energy of 190 eV. The ionization yield for 2ℓ electrons gives a photoionization cross section for the $n = 2$ subshell of 0.128 Mb, very similar to the result presented in [29]. The determination of a $1s$ photoionization cross section is more difficult. The Fourier transform of the electric field shows that the photon energy spectrum above the $1s$ ionization threshold accounts for about 2.3×10^{-5} of the full intensity. It contains three main components: 20% of the intensity associated with the photon energy spectrum above the $1s$ ionization threshold is found within 20 eV of the threshold, 70% of the intensity is associated with photon energies around 320 eV, and 10% with photon energies around 365 eV. If we assume that the full $1s$ emission yield arises from photon energies around 320 eV, a cross section of 0.64 Mb is obtained, which compares reasonably well with a reported photoionization cross section of 0.86 Mb at a photon energy of 300 eV [29], given the various uncertainties in transforming the yield into a cross section.

Using the same procedure, we obtain a photoionization cross section of 0.070 Mb for the $n = 2$ subshell for a central photon energy of 245 eV, in good agreement with the result reported in [29]. The estimate of a $1s$ photoionization cross section is again more complicated. The Fourier transform of the electric field shows that the photon energy spectrum above the $1s$ ionization threshold accounts for 0.88% of the full intensity. It contains two main components: 33% of the intensity with photon energy above the $1s$ ionization threshold is found within 8 eV of the threshold, with the remaining

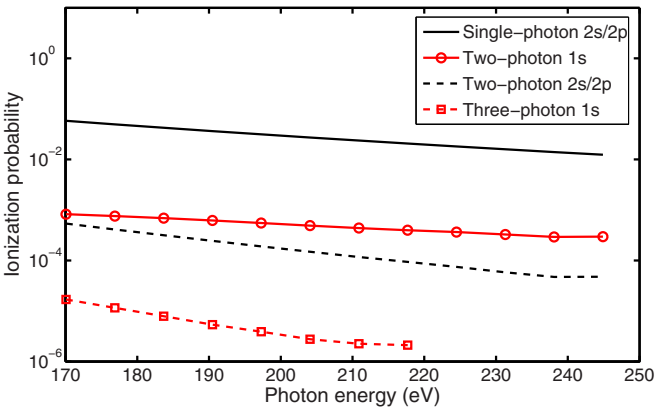

FIG. 1. (Color online) Yields for one- and two-photon emission of a 2ℓ electron and two- and three-photon emission of a $1s$ electron from neutral C irradiated by a short laser pulse with a peak intensity of 10^{17} W/cm^2 as a function of photon energy. The three-photon emission yield is estimated through subtraction of the single-photon yield induced by the edges of the pulse bandwidth. Data associated with this report can be accessed via [30].

67% of the intensity associated with photon energies peaking around 310 eV. If we assume that the full $1s$ emission yield arises from photon energies around 310 eV, a cross section of 0.31 Mb is obtained, which is nearly a factor of 3 smaller than the reported photoionization cross section of 0.86 Mb at a photon energy of 300 eV [29]. The reason for this increase in discrepancy is unknown. The components near threshold are strongest at threshold and may, therefore, not lead to ionization within the calculations, due to the time needed by the photoelectron to leave the inner region. However, this would only increase our estimate of the cross section to 0.46 Mb, which is still notably below the previous result. Other possible reasons for the discrepancy include the short duration of the pulse, and possible interference arising from excitation of the $1s$ electron to np states by the central component of the pulse.

Table I shows that, through consideration of the outer-region channels, we can obtain emission yields for single-photon emission of a $2s$ or $2p$ electron, two-photon emission of a $1s$ electron, two-photon emission of a $2s$ or $2p$ electron, and an approximation to three-photon emission yield of a $1s$ electron at lower photon energies at an intensity of 10^{17} W/cm^2. Figure 1 shows these emission yields as a function of photon energy. The figure demonstrates that multiphoton emission is not negligible at this intensity, as it contributes between 2% and 3% to the total emission. The figure demonstrates that two-photon emission of the inner $1s$ electron is more important than two-photon emission of an outer $2s$ or $2p$ electron, and the importance of two-photon emission of a $1s$ electron increases with photon energy, compared to both single-photon and two-photon emission of a 2ℓ electron. Three-photon emission of the $1s$ electron contributes about 0.02% to the total photoemission yield for a photon energy of 170 eV and an intensity 10^{17} W/cm^2. This contribution drops to about 0.01% at a photon energy of 210 eV.

At the highest intensity considered in the present calculation, 10^{18} W/cm^2, the increase in ionization yield no longer follows a perturbative scaling law. However, the relative

TABLE II. Populations of final states of C^+ after irradiation of a ground-state C atom by an eight-cycle laser pulse with an intensity of 10^{17} W/cm^2 at photon energies of 170, 197, and 224 eV. The notation 1.16(−2) denotes 1.16×10^{-2}.

C^+	Final-state population at a photon energy of		
state	170 eV	197 eV	224 eV
$1s^22s^22p\ ^2P^o$	1.16(−2)	5.35(−3)	2.64(−3)
$1s^22s2p^2\ ^4P^e$	3.07(−2)	1.70(−2)	9.98(−3)
$1s^22s2p^2\ ^2D^e$	4.92(−4)	2.12(−4)	1.11(−4)
$1s^22s2p^2\ ^2S^e$	7.47(−5)	3.43(−5)	2.03(−5)
$1s^22s2p^2\ ^2P^e$	1.24(−2)	7.24(−3)	4.43(−3)
$1s^22p^3\ ^4S^o$	9.92(−4)	5.07(−4)	2.88(−4)
$1s^22p^3\ ^2D^o$	1.55(−3)	7.81(−4)	4.29(−4)
$1s^22p^3\ ^2P^o$	8.29(−4)	4.40(−4)	2.51(−4)
$1s2s^22p^2\ ^4P^e$	4.90(−4)	3.56(−4)	2.29(−4)
$1s2s^22p^2\ ^2P^e$	2.91(−4)	1.74(−4)	1.08(−4)
$1s2s^22p^2\ ^2D^e$	9.27(−6)	8.80(−7)	2.52(−6)
$1s2s^22p^2\ ^2S^e$	3.18(−6)	1.61(−7)	3.58(−7)
$1s2s2p^3\ ^4S^o$	2.71(−6)	1.21(−6)	5.01(−6)
$1s2s2p^3\ ^4D^o$	9.94(−6)	8.06(−6)	8.43(−6)
$1s2s2p^3\ ^4P^o$	4.47(−6)	3.60(−6)	4.60(−6)
$1s2s2p^3\ ^2D^o$	1.12(−5)	4.66(−6)	2.85(−6)
$1s2s2p^3\ ^2P^o$	5.46(−6)	1.85(−6)	1.30(−6)
$1s2s2p^3\ ^2D^o$	3.51(−6)	1.03(−6)	2.63(−6)
$1s2s2p^3\ ^4S^o$	4.29(−6)	3.03(−6)	1.80(−6)
$1s2s2p^3\ ^2S^o$	1.62(−6)	1.23(−6)	2.48(−6)
$1s2s2p^3\ ^2P^o$	3.11(−6)	5.17(−7)	1.49(−6)
$1s2p^4\ ^4P^e$	4.59(−7)	2.85(−7)	3.37(−7)
$1s2p^4\ ^2D^e$	7.30(−7)	1.79(−7)	3.48(−7)
$1s2p^4\ ^2S^e$	3.48(−7)	7.21(−8)	2.09(−7)
$1s2p^4\ ^2P^e$	2.11(−7)	3.17(−8)	3.49(−8)

importance of higher-order processes continues to increase. At this intensity, two-photon emission of a $1s$ electron accounts for 16% of all photoemission processes, with two-photon emission of a 2ℓ electron accounting for another 2%. Therefore, at intensities approaching 10^{18} W/cm^2, a full analysis of the physics must account for the potential effects of absorption of more than just a single photon.

Previously, we investigated the competition between multiphoton absorption by a $1s$ and $2s$ electron from the initial $1s2s\ ^1S$ state in He [13]. In that study, it was found that at the two-photon level, the $1s$ electron was about five times as likely as the $2s$ electron to absorb two photons. In the present study, at 175 eV, the $1s$ electron is about 2.5 times as likely to absorb two photons than for a 2ℓ electron to absorb two photons, whereas it is a factor of 6 at a photon energy of 245 eV. The ratio obtained here is therefore comparable to the one found for He, even though in the present case, there are twice as many 2ℓ electrons as $1s$ electrons. On the other hand, as shown later, the emission of 2ℓ electrons is dominated by emission of a $2s$ electron, with $2p$ electrons contributing notably less.

The RMT calculations also provide the populations in the various residual C^+ states. Table II provides the final populations for all C^+ states included in the calculations for photon energies of 170, 197, and 224 eV at an intensity of 10^{17} W/cm^2. For the photon energies given in the table, effects due to the bandwidth of the pulse are expected to play only a minor role and should not affect the final populations significantly.

The table demonstrates that the main residual-ion states are the $1s^22s2p^2\ ^4P^e$ and $^2P^e$ states indicating a dominance of direct emission of a $2s$ electron. Emission of a $2p$ electron accounts for 20% of the emission processes at 170 eV and only 14% at 224 eV. C^+ is left in a $1s^22p^3$ state in about 5.2–5.7% of all emission processes. This latter outcome is only a factor of 4 more likely than the emission of an inner $1s$ electron, which occurs in 1.4–2.0% of all emission processes.

In addition, Table II shows that the emission of the inner electrons can involve the outer electrons. The outer electrons are left in a $2s^22p^2$ configuration in 91–93% of all $1s$ emission processes. However, the final distribution over the $1s2s^22p^2$ shows deviations from the statistical distribution of a 2:1 ratio between the $^4P^e$ and the $^2P^e$ state, with a 5:3 ratio at 170 eV and a ratio of 2.1:1 at a photon energy of 224 eV. In 7–9% of the $1s$ ionization processes, a change in the outer electron population occurs, mainly an excitation of a $2s$ electron to $2p$. This suggests that in just under 10% of the processes, two different electrons absorb a photon. Hence, this provides a signature of a multielectron response to the light field, which may involve a sequential process, whereby the first photon excites a $1s$ electron to $2p$, followed by photoemission of one of the $2s$ electrons.

The table demonstrates that all emission processes involving an outer $2s$ or $2p$ electron decrease in magnitude with increasing photon energy. However, this pattern changes when a $1s$ electron is emitted. Although the population in the dominant residual-ion states after emission of a $1s$ electron ($1s2s^22p^2\ ^2P^e$ and $^4P^e$) shows a decrease in final population with increasing photon energy, for the other $1s2s^22p^2$ states, for five out of nine $1s2s2p^3$ residual-ion states and all $1s2p^4$ states, the final population is larger at a photon energy of 224 eV than at a photon energy of 197 eV. This could be due to an intermediate resonance, but it could also originate from the closer proximity of the threshold for single-photon emission of a $1s$ electron at this higher photon energy.

To investigate the origin of the increase, we have carried out further calculations of inner-shell photoemission of C atoms covering the photon-energy range between 170 and 245 eV. Outcomes of these calculations are shown in Fig. 2. To maintain clarity, the figure shows the probability that the C^+ ion is left in a particular configuration, rather than in individual states within the configuration. Most residual C^+ ions are left in the $1s^22s2p^2$ configuration, indicating that emission of a $2s$ electron is the most likely photoionization process. The probability of emission of a $2p$ electron is about a factor of 4 times smaller at 170 eV, and this probability decreases with increasing photon energy. The probability that the C^+ ion is left in $1s^22p^3$ is over an order of magnitude smaller than the probability for emission of a $2s$ electron. Emission of a $1s$ electron preferentially leaves the C^+ ion in the $1s2s^22p^2$ configuration, accounting for about 2% of the photoionization processes at 170 eV. This probability increases beyond 230 eV, and reaches about 5% for 245 eV. This increase at the highest photon energies can be ascribed to the increasing proximity of the threshold for single-photon emission of the $1s$ electron.

Figure 2 shows that the probability of leaving the residual C^+ ion in the $1s2s2p^3$ and $1s2p^4$ configurations are resonantly

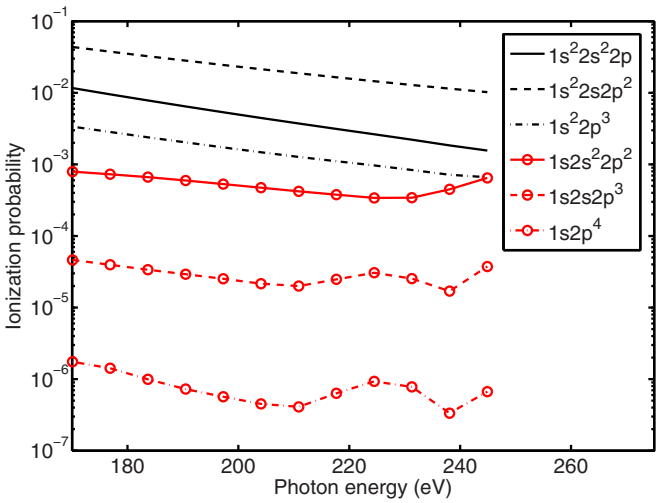

FIG. 2. (Color online) Photoionization yields for residual-ion configurations of C^+ as a function of photon energy at an intensity of 10^{17} W/cm^2.

enhanced at a photon energy of 224 eV. The populations in the $1s2s^22p^2$ configuration show an enhancement near the threshold for single-photon emission of a $1s$ electron, but this enhancement only becomes noticeable above a photon energy of 230 eV. The most likely origin of the enhancement is the intermediate $1s2s^22p^3$ configuration reached by photoexcitation of a $1s$ electron into the $2p$ shell. The ultrashort duration of the pulse means that the effect of the intermediate configuration is apparent over a broad photon energy range with very little structure. Since the effects of the resonances are spread out over a broad photon energy range, the overall increase in the ionization probability will be reduced, and as a consequence resonant enhancement is only visible for the weakest photoionization channels.

IV. CONCLUSIONS

In conclusion, we have demonstrated the capability of RMT theory to investigate ultrafast inner-shell emission processes in general multielectron atoms. Two-photon emission of a $1s$ electron from C atoms was investigated in the photon energy range between 175 and 245 eV. At an intensity of 10^{17} W/cm^2, two-photon emission of the $1s$ electron accounts for about 2–3% of all photoionization processes. At the two-photon level, emission of the $1s$ electron is about a factor of 2 more likely than the emission of either a $2p$ or a $2s$ electron combined. Through examination of the final configuration of the residual C^+ ion, we have furthermore observed evidence for resonant enhancement of the $1s$ emission. Finally, by comparing ionization yields in different symmetries across multiple intensities, we have determined an above-threshold ionization yield for inner-shell photoemission of the $1s$ electron in C.

The determination of inner-shell processes in general multielectron atoms poses a number of challenges. The present calculations have been carried out using Hartree-Fock orbitals for ground-state C. The description of the residual ion states can be improved by expanding the initial orbital set to include pseudo-orbitals. However, the inclusion of pseudo-orbitals will lead to significantly larger calculations. The main reason for this is that residual-ion states are retained in the present R-matrix calculations in order of energy. The lowest-energy states will be dominated by states with two $1s$ electrons. These states can involve the Hartree-Fock $2s$ and $2p$ orbitals, but may also involve the additional pseudo-orbitals. Hence, a significant number of states dominated by pseudo-orbitals may have to be included before one reaches the ionic states corresponding to emission of a $1s$ electron. Furthermore, the calculations require a good description of the continuum up to high energy. This leads to much higher energies associated with the Bloch operator. The higher energies reached in the present calculations do not yet affect the stability of the RMT approach.

A further open question concerns the influence of nondipole terms. The present study assumes that the dipole approximation holds. This approximation is not unreasonable for the interaction between the laser field and the $1s$ orbital. However, the approximation may not be as suitable for describing the interactions between the 2ℓ electrons and the laser field. The investigation of nondipole effects would require substantial computational development. The RMT codes themselves will need to be modified to ensure that all relevant interactions arising from the laser field are properly taken into account. More importantly, the inner-region R-matrix codes need modification so that higher-order transitions are calculated within the inner region, and generated in a form suitable for use within the RMT codes.

ACKNOWLEDGMENTS

The authors wish to thank A.C. Brown and J.S. Parker for valuable assistance. This work was supported by the UK EPSRC under Grant No. EP/G055416/1 and the EC Initial Training Network CORINF. This work used the ARCHER UK National Supercomputing Service (http://www.archer.ac.uk).

[1] J. Feldhaus, M. Krikunova, M. Meyer, Th. Möller, R. Moshammer, A. Rudenko, Th. Tschentscher, and J. Ullrich, J. Phys. B **46**, 164002 (2013).
[2] C. Bostedt *et al.*, J. Phys. B **46**, 164003 (2013).
[3] M. Yabashi *et al.*, J. Phys. B **46**, 164001 (2013).
[4] M. Meyer *et al.*, Phys. Rev. Lett. **104**, 213001 (2010).
[5] B. Rudek *et al.*, Nat. Photonics **6**, 858 (2012).
[6] T. Sato *et al.*, Appl. Phys. Lett. **92**, 154103 (2008).
[7] M. Tilley, A. Karamatskou, and R. Santra, J. Phys. B **48**, 124001 (2015).
[8] B. Cooper, P. Kolorenč, L. J. Frasinski, V. Averbukh, and J. P. Marangos, Faraday Discuss. **171**, 93 (2014).

[9] H. F. Rey and H. W. van der Hart, Phys. Rev. A **90**, 033402 (2014).
[10] E. Plésiat, L. Argenti, E. Kukk, C. Miron, K. Ueda, P. Decleva, and F. Martín, Phys. Rev. A **85**, 023409 (2012).
[11] F. Silva, S. M. Teichmann, S. L. Cousin, M. Hemmer, and J. Biegert, Nat. Commun. **6**, 6611 (2015).
[12] H. W. van der Hart, Phys. Rev. Lett. **95**, 153001 (2005).
[13] M. Madine and H. W. van der Hart, J. Phys. B **38**, 3963 (2005).
[14] L. A. A. Nikolopoulos, J. S. Parker, and K. T. Taylor, Phys. Rev. A **78**, 063420 (2008).
[15] M. A. Lysaght, L. R. Moore, L. A. A. Nikolopoulos, J. S. Parker, H. W. van der Hart, and K. T. Taylor, *Quantum Dynamic Imaging: Theoretical and Numerical Methods*, edited by A. D. Bandrauk and M. Yu. Ivanov (Springer, New York, 2011), pp. 107–134.
[16] L. R. Moore, M. A. Lysaght, L. A. A. Nikolopoulos, J. S. Parker, H. W. van der Hart, and K. T. Taylor, J. Mod. Opt. **58**, 1132 (2011).
[17] H. W. van der Hart, M. A. Lysaght, and P. G. Burke, Phys. Rev. A **76**, 043405 (2007).
[18] X. Guan, O. Zatsarinny, K. Bartschat, B. I. Schneider, J. Feist, and C. J. Noble, Phys. Rev. A **76**, 053411 (2007).
[19] P. G. Burke, *R-Matrix Theory of Atomic Collisions* (Springer-Verlag, Heidelberg, 2011).
[20] E. S. Smyth, J. S. Parker, and K. T. Taylor, Comput. Phys. Commun. **114**, 1 (1998).
[21] O. Hassouneh, A. C. Brown, and H. W. van der Hart, Phys. Rev. A **90**, 043418 (2014).
[22] K. Bartschat, E. T. Hudson, M. P. Scott, P. G. Burke, and V. M. Burke, J. Phys. B: At. Mol. Opt. Phys. **29**, 115 (1996).
[23] N. S. Scott, M. P. Scott, P. G. Burke, T. Stitt, V. Faro-Maza, C. Denis, and A. Maniopoulou, Comput. Phys. Commun. **180**, 2424 (2009).
[24] H. W. van der Hart, Phys. Rev. A **89**, 053407 (2014).
[25] J. Wragg, J. S. Parker, and H. W. van der Hart, Phys. Rev. A (to be published).
[26] M. A. Lysaght, H. W. van der Hart, and P. G. Burke, Phys. Rev. A **79**, 053411 (2009).
[27] E. Clementi and C. Roetti, At. Data. Nucl. Data Tables **14**, 177 (1974).
[28] S. Hutchinson, M. A. Lysaght, and H. W. van der Hart, J. Phys. B **43**, 095603 (2010).
[29] J. J. Yeh and I. Lindau, At. Data Nucl. Data Tables **32**, 1 (1985).
[30] http://pure.qub.ac.uk/portal